

Flow Visualization and Characterization of an Artery Model with Stenosis

Anis S. Shuib, Peter R. Hoskins and William J. Easson

Abstract—Cardiovascular diseases, principally atherosclerosis, are responsible for 30% of world deaths. Atherosclerosis is due to the formation of plaque. The fatty plaque may be at risk of rupture, leading typically to stroke and heart attack. The plaque is usually associated with a high degree of lumen reduction, called a stenosis. It is increasingly recognized that the initiation and progression of disease and the occurrence of clinical events is a complex interplay between the local biomechanical environment and the local vascular biology. The aim of this study is to investigate the flow behavior through a stenosed artery. A physical experiment was performed using an artery model and blood analogue fluid. An axisymmetric model constructed consists of contraction and expansion region that follow a mathematical form of cosine function. A 30% diameter reduction was used in this study. The flow field was measured using particle image velocimetry (PIV). Spherical particles with 20 μ m diameter were seeded in a water-glycerol-NaCl mixture. Steady flow Reynolds numbers are 250. The area of interest is the region after the stenosis where the flow separation occurs. The velocity field was measured and the velocity gradient was investigated. There was high particle concentration in the recirculation zone. High velocity gradient formed immediately after the stenosis throat created a lift force that enhanced particle migration to the flow separation area.

Keywords—Stenosis artery, Biofluid mechanics, PIV

I. INTRODUCTION

ATHEROSCLEROSIS is one of cardiovascular disease and described as the build-up of fatty materials in the inner wall of the arteries. The narrowing of the arterial lumen is called a stenosis. If the degree of vessel occlusion is severe, this prevents sufficient oxygen and nutrition reaching the distal tissues resulting in tissue damage and tissue death. Atherosclerotic lesions, which initiated in low wall shear stress region [1] grow over time and form a plaque with high concentration of lipid. The sites of stenotic diseases are commonly found in the cerebral artery, the femoral artery, the abdominal aorta and the carotid bifurcation. The common features of these arteries include curvature and bifurcation where secondary flow and recirculation might develop and consequently change the fluid loading on vessel walls [2]. Table I presents the characteristic values of flow parameters within major healthy arteries where the vessel mean diameter and the time-averaged Reynolds number, Re are tabulated [3].

A. S. Shuib is with the Universiti Teknologi Petronas, Malaysia (phone: 605-368-7574; fax: 605-365-6176; e-mail: anisuha@petronas.com.my).

P. R. Hoskins is with the Department of Medical Physics, University of Edinburgh, UK (e-mail: p.hoskins@ed.ac.uk).

W. J. Easson is with Institute for Materials and Processes, University of Edinburgh, UK (e-mail: bill.easson@ed.ac.uk).

Re describes the ratio of inertial to viscous forces in fluid. Re is proportional to the magnitude of the inertia force to the viscous force. In general the flow Re of fluid in the cylindrical geometry is defined as

$$Re = \frac{\rho D v}{\mu} \quad (1)$$

where ρ denotes the density of the fluid, D is the inlet diameter of the tube, v is the mean inlet velocity of the fluid, and μ is the viscosity of the fluid.

Stenotic flows have been extensively studied over a wide range of flow conditions. The Reynolds number, Re has ranged between 1800~2300 [4] and 15000 [5]. Ahmed and Giddens [6] have performed studies in the range of 500 to 2000. Physiological flows for medium-size arteries are well below this range: normally between 100 and 2000 [7]. The mean flow Re in the carotid artery was around 300 [8]. Arterial disease progresses due to an interplay between local mechanical forces and local biology. Characterization of flow is important in order to understand the effect of hydrodynamics on the development and progression of the disease. This paper presents the characterization of flow field in a stenosed artery model. The velocity is determined by PIV method and the velocity gradient is calculated.

TABLE I
REYNOLDS NUMBER IN HUMAN ARTERIES [3]

| Vessel | Mean diameter (mm) | Re |
|---------------------------|--------------------|------|
| Femoral artery | 5.0 | 280 |
| Common carotid | 5.9 | 330 |
| Internal carotid | 6.1 | 220 |
| Left main coronary artery | 4.0 | 240 |
| Right coronary | 3.4 | 150 |

II. EXPERIMENTAL SYSTEM AND TECHNIQUES

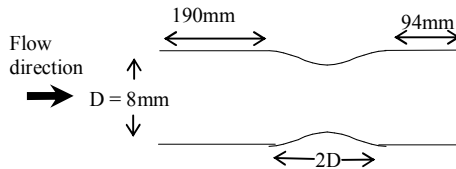
Detail experimental technique has been discussed in a separate paper [9]. The following section will highlight the method used in this experiment.

A. Stenosis Artery Model

An axisymmetric stenosis model was manufactured from silicone rubber (Sylgard 184, Dow Corning) using 'lost core' technique[10]. The resultant shape of the stenosis phantom with 30% diameter reduction was shown in Fig. 1. The inlet diameter of the tube, D was 8mm and the entrance length immediately before and after the stenosis were 190mm and 94mm respectively. The axial length in the stenosis region was $2D$.



(a) Stenosis artery model



(b) Schematic diagram of the model (not to scale)

Fig. 1 Stenosed artery model 30% diameter reduction

The flow of the fluid was steady and driven by a peristaltic pump (Masterflex L/S, Cole-Parmer Instrument) through a pulse dampener before entering the stenosis artery model. The mean at inlet was 0.18m/s or equivalent to Reynolds number, Re of 250.

B. Fluid Suspension

The fluid consists of particles suspended in liquid. The liquid was formulated to have a refractive index matched to the flow phantom material. The compositions of the liquid by weight were glycerol 37.1%, water 47.9% and NaCl 15.0%. The refractive index of both liquid and the silicone model was 1.41. The viscosity of the liquid solution was 6.23 ± 0.01 mPas and the density was 1080 kg/m^3 . The particles chosen were spherical rigid particles made from polyamide material (Orgasol, Elf-atochem, France). The density of the particle was 1030 kg/m^3 hence it was assumed neutrally buoyant. The properties were summarized in Table II and Table III. The particles size was $20 \pm 2 \mu\text{m}$ diameter. The weight of particles was measured and then mixed with glycerol-water-NaCl solution. Particles concentrations, ϕ_m of 0.14% by weight were prepared. The particle suspension was stirred for 30 minutes and filtered to remove remaining clumps. The distribution of particles in the solution was observed under microscope (Zeiss, Germany) to ensure particles were not aggregate and moved as a single particle in the fluid. The temperature was kept constant at 20°C .

TABLE II
FLUID PROPERTIES

| Compositions (w/w%) | Viscosity, μ | Density, ρ |
|---------------------|----------------------|-----------------------|
| Glycerol = 37.1 | 6.23 ± 0.01 mPas | 1080 kg/m^3 |
| Water = 47.9 | | |
| NaCl = 15.0 | | |

TABLE III
PARTICLES PROPERTIES

| | |
|-------------------------|--|
| Material | Polyamide (Orgasol) |
| Shape | Rigid, roughly sphere |
| Diameter, d_p | $20 \pm 2 \mu\text{m}$ |
| Density, ρ_p | 1030 kg/m^3 |
| Concentration, ϕ_m | 0.14 % (by weight percent in solution) |

C. Flow Measurement

A particle image velocimetry (PIV) system (Dantec Dynamics Ltd., UK) was used to acquire the images of particle distribution in the flow. From the images recorded, the velocity vector is calculated. The PIV set-up consisted of an Nd:YAG pulsed laser (Newwave Solo 200XT) of wavelength 532nm with repetition rate between 8 to 21Hz, a high speed digital camera (Kodak Megaplug ES 1.0) with maximum of 15 frame per second for double frame mode and a computer interface (FlowMap, Dantec Dynamics, UK). The set-up is shown in Fig. 2. With flow illuminated, the camera acquired images of the flow field. The area of interest was at the expansion section of the stenosed artery.

Post processing of the data was performed using FLOWMANAGER (Dantec Dynamics Ltd., UK) and MATLAB r2009a (The Mathworks, US).

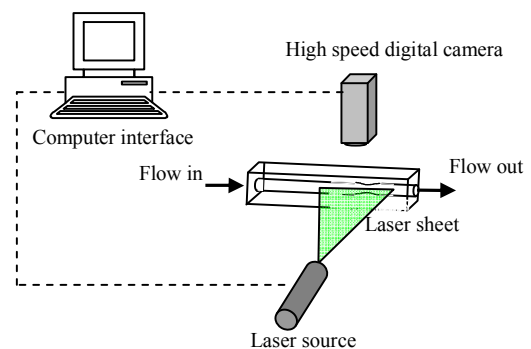


Fig. 2 Schematic representation of the PIV setup

III. RESULTS AND DISCUSSIONS

Normalized geometrical coordinates is used to discuss the results. The coordinates is shown in Fig. 3. The radial coordinate was normalised by the inlet geometry radius, R (4mm) and the axial coordinate by the diameter, D (8mm).

The coordinates' reference point (0,0) lay in the central coordinate of the throat region.

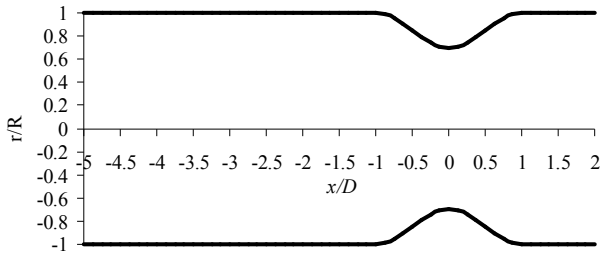


Fig. 3 Normalized scale

The flow field at the post stenosis region at $Re=250$ measured by particle image velocimetry is shown in Fig. 4. The velocity vectors are imposed onto the image. The vector's reference scale was equivalent to 0.2m/s. The background image corresponds to the average light intensity of 200 images. In this frame size, 1008x1016 pixels equalled 8.2x8.3 millimetres. In general, the flow was laminar through distal and proximal to the stenosis. For the velocity field at the corner of the stenosis, there was relatively high scattered light intensity near the wall. The enlargement of this region is shown in Fig. 5. The vectors clearly indicate flow recirculation.

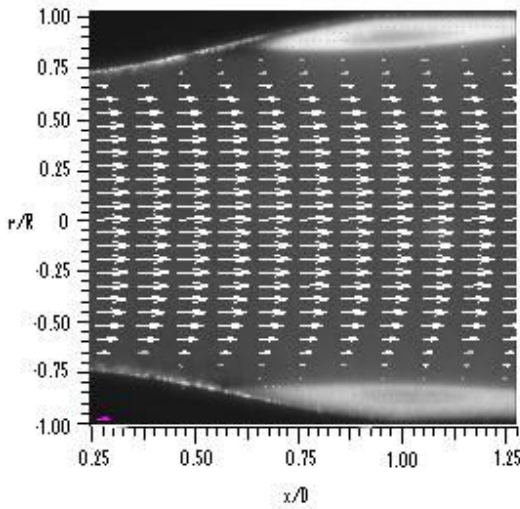


Fig. 4 Vector field distal to stenosis

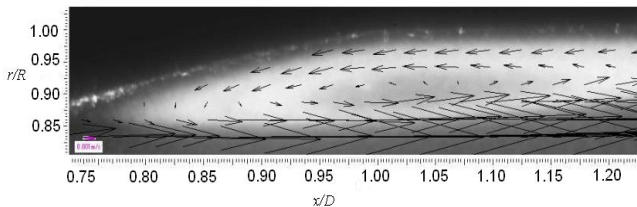


Fig. 5 Enlargement of velocity vector at the corner of stenosis

The velocity magnitude is shown in Fig. 6, where the axial velocity of is plotted. The negative magnitude near the wall indicates the reversed flow.

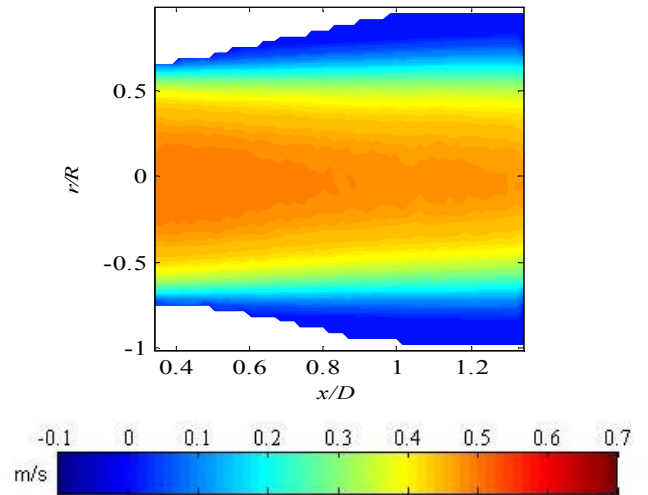


Fig. 6 Velocity plot

The recirculation formed was due to sudden change in the cross-sectional area at the throat of the stenosis, the velocity increased and the pressure dropped at a faster rate. This was accompanied by a jet formation. The flow Re here was 30% higher than at the inlet. In the expansion section, the decrease in velocity was accompanied by an increase in static pressure in the direction of motion. The adverse pressure tended to retard the flow. In the mainstream, the inertia opposed the retardation but close to the wall, the fluid velocity and inertia were smaller. The fluid lost momentum due to viscous friction; hence, it was decelerated by the adverse pressure gradient and the direction of flow was inverted. Boundary-layer separation occurred and fluid recirculation was observed between the jet and the wall. This site produced most of the lost pressure, thus creating additional viscous loss. The results of the experiment agree well with the observations of Ku [2], Berger and Jou [11], and Wootton and Ku [12]. Fig. 7 depicts the velocity gradient, du/dr . At the centreline, the velocity gradient is always zero. At the inlet, the gradient increased towards the wall. The velocity gradient between $r/R = 0.5$ and 0.7 is higher than that of the recirculation region. As the flow moves downstream these gradients decrease.

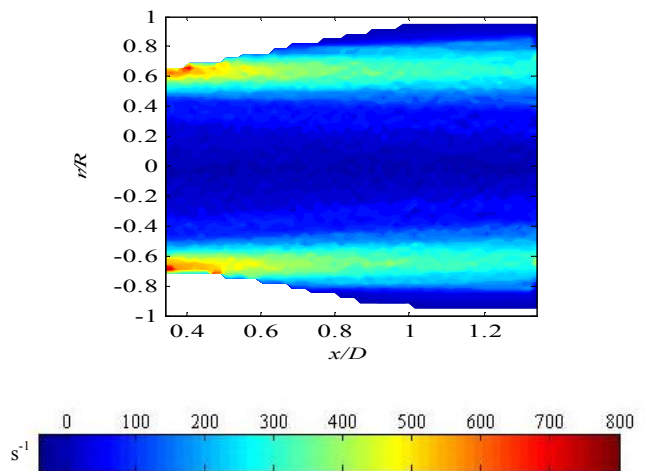


Fig. 7 Velocity gradient

High intensity of particles scattered in the recirculation region could be explained in terms of shear gradient observed. More particles migrated to the recirculation region where the shear gradient is low. Lift forces is significant where the shear gradient is high [8]. In the high shear region, the particles may have rotated due to pressure gradient induced by velocity different at the top and bottom of the particles. As a result, the particles migrated from the high shear region and reside in the low shear zone.

In arteries, the interaction between blood cells, low density lipoproteins and muscle cells could result in the progression of atherosclerosis. Hence, the mechanism triggering atherosclerosis plaque build-up might be enhanced where the concentration of blood cells was high while orbiting in the recirculation zone.

IV. CONCLUSION

This study demonstrated the importance of flow characterization and visualization in order to understand the flow in diseased artery. The flow at $Re=250$ is streamlined and laminar. The particle concentration in the flow separation region indicated by the light intensity was significantly higher. High concentration of particles in the recirculation can be related to the shear gradient. Particles migrated from the high shear region to recirculation zone. This phenomenon suggested a physiological impact on the progression of atherosclerosis. Further experiments are recommended to look at more realistic physiological condition such as pulse flow, the properties and concentration of particles.

REFERENCES

- [1] C. G. Caro, J. M. Fitz-Gerald, and R. C. Schroter, "Atheroma and arterial wall shear. Observation, correlation and proposal of a shear dependent mass transfer mechanism for atherogenesis," *Proc Royal Soc Lond Biol Sci*, vol. 177, pp. 109-159, 1971.
- [2] D. N. Ku, "Blood flow in arteries," *Annual Review Of Fluid Mechanics*, vol. 29, pp. 399-434, 1997.
- [3] J. J. Hathcock, "Flow effects on coagulation and thrombosis," *Arteriosclerosis Thrombosis and Vascular Biology*, vol. 26, no. 8, pp. 1729-1737, Aug, 2006.
- [4] D. P. Giddens, C. K. Zarins, and S. Glagov, "The Role Of Fluid-Mechanics In The Localization And Detection Of Atherosclerosis," *Journal Of Biomechanical Engineering-Transactions Of The Asme*, vol. 115, no. 4, pp. 588-594, Nov, 1993.
- [5] M. D. Deshpande, and D. P. Giddens, "Turbulence Measurements in a Constricted Tube," *Journal of Fluid Mechanics*, vol. 97, no. MAR, pp. 65-89, 1980.
- [6] S. A. Ahmed, and D. P. Giddens, "Velocity-Measurements in Steady Flow through Axisymmetric Stenoses at Moderate Reynolds-Numbers," *Journal of Biomechanics*, vol. 16, no. 7, pp. 505-&, 1983.
- [7] C. G. Caro, *The mechanics of the circulation*, Oxford: Oxford University Press, 1978.
- [8] Q. Long, X. Y. Xu, K. V. Ramnarine *et al.*, "Numerical investigation of physiologically realistic pulsatile flow through arterial stenosis," *Journal of Biomechanics*, vol. 34, no. 10, pp. 1229-1242, 2001.
- [9] A. Shuib, P. Hoskins, and W. Easson, "Experimental investigation of particle distribution in a flow through a stenosed artery," *Journal of Mechanical Science and Technology*, vol. 25, no. 2, pp. 357-364, 2010.
- [10] J. R. Blake, W. J. Easson, and P. R. Hoskins, "A Dual-Phantom System for Validation of Velocity Measurements in Stenosis Models Under Steady Flow," *Ultrasound in Medicine & Biology*, vol. 35, no. 9, pp. 1510-1524, 2009.
- [11] S. A. Berger, and L. D. Jou, "Flows in stenotic vessels," *Annual Review of Fluid Mechanics*, vol. 32, pp. 347-382, 2000.
- [12] D. M. Wootton, and D. N. Ku, "Fluid mechanics of vascular systems, diseases, and thrombosis," *Annual Review Of Biomedical Engineering*, vol. 1, pp. 299-329, 1999.